ChemComm

Accepted Manuscript

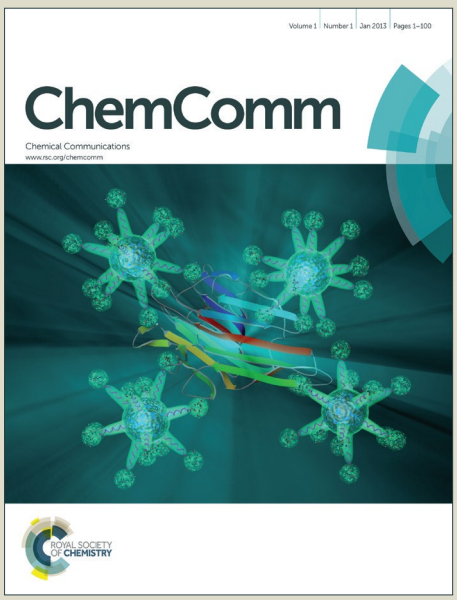

ROYAL SOCIETY OF CHEMISTRY

www.rsc.org/chemcomm

Journal Name

COMMUNICATION

Nanostructured High-Performance Dielectric Block Copolymer

Wenmei Liu,[a] Xiaojuan Liao,[a] Yawei Li,[b] Qiuhua Zhao,[a] Meiran Xie*[a] and Ruyi Sun*[a]

Received 00th January 20xx,
Accepted 00th January 20xx

DOI: 10.1039/x0xx00000x

www.rsc.org/

A new type of insulating-conductive block copolymer was synthesized by metathesis polymerizations, self-assembled into unique nanostructure of micelle or hollow sphere, and exhibited high dielectric constant, low dielectric loss, and high stored/released energy density by combining the strong dipolar and nano-interfacial polarizations.

Dielectric materials with high dielectric constant, high energy density, and minimum dielectric loss are attractive and strongly desirable for film capacitor and pulsed power application.[1-3] Polymers and polymer composites have some advantages such as flexibility, higher breakdown strength, and lower dielectric loss over inorganic ceramic materials (e.g. barium titanate).[4] Unfortunately, most polymers usually possess low dielectric constant (2-5); although poly(vinylidene fluoride)-based ferroelectric polymers[3,5] can offer relatively high dielectric constant (≥10), they exhibit high dielectric loss due to hysteresis that accompanies the orientational polarization of the polymers' large crystalline domains. Dielectric performance of polymers was affected by four type of polarizations including electronic, orientational (or dipolar), ionic, and interfacial polarizations,[6] and some of them have been used to improve the dielectric properties. Introducing functional groups with large dipole moment, such as the polar F and nitrile-contained groups, is a common approach to increase the orientational polarization;[7] the construction of inorganic/organic polymer composites makes use of the high orientational polarization of inorganic ceramic;[8] the percolative dielectric composites, depending on the interfacial polarization between conductive fillers (e.g. metal particles) and insulating polymer matrix, have caused a great attention for their high dielectric constants when the contents of conductive fillers close to the threshold.[9] Recently, lots of new structures[5c,10] and conductive fillers including polyaniline,[11] polythiophene,[12] graphene,[13] and carbon nanotubes[14] were used, expecting to improve the dispensability of conductive segments, enhance the compatibility of composite components, and ultimately decrease dielectric dissipation and the frequency dependency. However, it is still a challenging task for preparing polymers or polymer composites with high dielectric constant and low dielectric loss. The covalent–linkage between the conductive and insulating moieties could be benefit to improve the compatibility and result in low dielectric loss.[15] Combining multiple polarization and constructing a unique nanostructure are envisioned to further promote the dielectric properties of polymers.

Polynorbornenes, known as the insulated low-dielectric materials[16] and prepared by ring-opening metathesis polymerization (ROMP), can be functionalized by the introduction of polar side groups to greatly increase the dielectric constant.[7,17] Besides, with stereoregular chain configuration, the accumulation of dipole can also enhance dielectric constant.[18] Polyacetylene (PA), the simplest conductive polymer, possesses an intrinsic conductivity of 10^{-9} (*cis*) to 10^{-5} (*trans*) S cm^{-1}, yet suffers from extremely low solubility and sensitivity to air. However, PAs with cyclic recurring units, prepared by metathesis cyclopolymerization (MCP),[19] display improved solubility and stability. Meanwhile, PA-contained copolymer also has better properties.[20] Since the high electrical conductivity of doping PA was reported,[21] a number of publications dealing with chemical, physical, and electrical properties of PA have appeared,[22] yet the dielectric property of PA-contained polymers has seldom studied. Herein, we report for the first time a dielectric-percolative block copolymer, poly(N-3,5-bisfluorophenyl-norbornen-pyrrolidine)-*block*-poly(4-pentafluorophenyl formate-1,6-heptadiyne) (**PFNP**-*b*-**PFHD**), with micelle or hollow sphere nanostructure, which will endow this material excellent dielectric properties.

Polymers poly(N-3,5-difluorophenyl-norbornene-dicarboximide) (**PFNDI**), **PFNP**, **PFHD**, and **PFNP**-***b***-**PFHD** were synthesized by ROMP, MCP, and tandem ROMP-MCP, respectively (Table S1, ESI†). The chemical structure and component of polymers were characterized by IR, NMR, UV–vis spectroscopy, and elemental analysis (Fig. S3-S7, Table S2, ESI†). The results indicated that **PFNP**-*b*-**PFHD** has all-*trans* and five-membered ring microstructure,[23] which may be benefit to elevate the dielectric constant.

[a] School of Chemistry and Molecular Engineering, East China Normal University, Shanghai 200241, China. E-mail: mrxie@chem.ecnu.edu.cn, rysun@chem.ecnu.edu.cn
[b] Key Laboratory of Polar Materials and Devices, Ministry of Education, Department of Electronic Engineering, East China Normal University, Shanghai 200241, China.
Electronic Supplementary Information (ESI) available: Experimental details and additional supportive data. See DOI: 10.1039/x0xx00000x

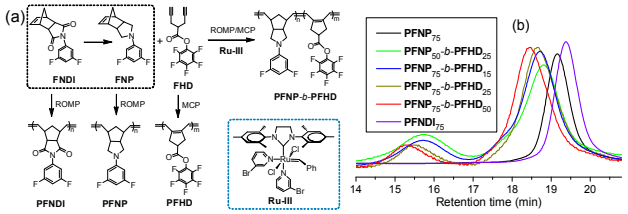

Fig. 1 Synthetic routes (a) and GPC traces (b) of homo- and copolymers.

Interestingly, GPC traces of copolymers showed two distinguished sets of curves (Fig. 1b). The major peak is in good accompany with the molecule weight (M_n) of single chain, whereas the minor trace with much higher M_n may be corresponded to the aggregates of about 10 chains ($M_{n,aggregate}$≈10$M_{n,single}$, Table S1, ESI†), demonstrating the self-assembly of copolymers proceeded in selective solvent without need for any post-treatments, such as dialysis or changing the specific solvent composition, which are essential for inducing the conventional self-assembly process; while no aggregates observed for homopolymer. This is an indicative of intriguing self-assembly driven by two elements: the solubility discrepancy of two blocks tends to make insoluble **PFHD** block aggregation away from THF; the π-π stacking and van der Waal interaction between the aromatic side chains and the rigid PA backbones make **PFHD** block close to each other in order. The self-assembly of copolymers was verified by DLS technique, revealing the aggregates existed in solution in different size (Fig. S8, ESI†). Under the action of these two driven forces synergistically, copolymer film would maintain the morphology in solution.

Further insight into the self-assembled morphology of copolymer film formed by solvent evaporation in air was carried out through TEM analysis. At a diluted condition (0.005 mg mL^{-1}), below the critical concentration of π-π stacking, the self-assembly of copolymers was only driven by the solubility discrepancy of blocks in solution, and **PFNP$_{75}$-*b*-PFHD$_{50}$** exhibited a micelle structure comprising insoluble, conductive **PFHD** segments as core and soluble, insulated **PFNP** segments as shell with a diameter of 37 nm (Fig. 2a). When the concentration increases to 0.05 mg mL^{-1}, the π-π stacking start to play a part and some of micelles re-assemble to form higher dimension hollow sphere to lowering the surface energy; the related wall thickness of hollow sphere is about 35 nm (Fig. 2b), which is nearly the same as the diameter of the primary micelle. As the concentration further increased to 0.2 mg mL^{-1}, more micelles transformed to hollow spheres and start to coalesce into larger hollow sphere with a diameter of 200 nm and a wall thickness of 60 nm (Fig. 2c). The morphology forming process was schematically illustrated in Fig. 2g. For copolymers with a fixed **PFNP** length of 75 units and elongated **PFHD** lengths from 15 to 50 units, the diameters of these hollow spheres in THF are almost the same (200 nm), but the wall thickness reduced from 90 nm to 60 nm at 0.2 mg mL^{-1} (Fig. 2d-2f). Since the soluble **PFNP** chain loosely packed around, the determining factor of the nanostructure size is the length of **PFNP**. As **PFHD** length increasing, the spherical micelle structure is not sufficient to cover the extended **PFHD** core, and the **PFHD** blocks take a closer alignment to avoid being solvated. The denser and in-order arrangement of **PFHD** block renders little change in size, but significantly thinning in wall thickness. Meanwhile, this more ordered arrangement in copolymers with a longer **PFHD** block was demonstrated by the presence of diffraction stripe in HR-TEM image (insert in Fig. 2a), which only can be seen in the dark region of **PFHD** core with 50 **FHD** units in backbone and other copolymers are amorphous. However, XRD analysis for all copolymers showed the same broad diffraction peak at 0.49 nm (Fig. S9, ESI†), which is corresponded to the π-π interaction, indicating the orderly packing did not induce obvious crystallization. DSC analysis also supported the conclusion since copolymers exhibited no crystallization during the cooling process, but displayed an increasing glass transition temperature (T_g) as **PFHD** block enlongated (Fig. S10, ESI†).

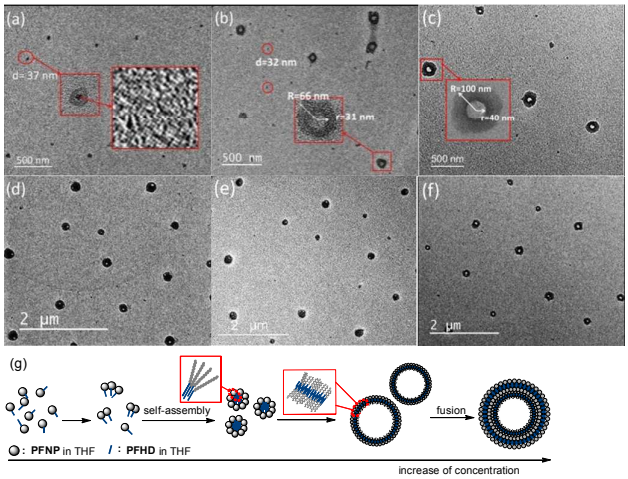

Fig. 2 TEM images of **PFNP$_{75}$-*b*-PFHD$_{50}$** at (a) 0.005 (insert: HR-TEM image), (b) 0.05, and (c) 0.2 mg mL^{-1} in THF. TEM images of (d) **PFNP$_{75}$-*b*-PFHD$_{15}$**, (e) **PFNP$_{75}$-*b*-PFHD$_{25}$**, and (f) **PFNP$_{75}$-*b*-PFHD$_{50}$** at 0.2 mg mL^{-1} in THF; (g) the schematic process of hollow sphere nanostructure from a single chain of copolymer in THF.

Surprisingly, by changing solvent to $CHCl_3$, TEM image showed uniformed micelle rather than hollow sphere with a diameter of 30 nm (Fig. S11a, ESI†) for **PFNP$_{75}$-*b*-PFHD$_{50}$** at 0.005 mg mL^{-1}. At 0.05 mg mL^{-1}, several larger particles with a diameter of about 100 nm appeared due to the micelle agglomeration driven by the π-π interaction and solvent evaporation, while most of the small micelles still remained (Fig. S11b, ESI†). Since the two blocks were linked by covalent bond, **PFHD** segments are hard to connect even though the micelles aggregated. After further increasing to 0.2 mg mL^{-1}, the number of larger aggregates increased with nearly the same size for **PFNP$_{75}$-*b*-PFHD$_{50}$**, **PFNP$_{75}$-*b*-PFHD$_{25}$**, and **PFNP$_{75}$-*b*-PFHD$_{15}$** (Fig. S11c-S11e, Scheme S1, ESI†). In general, the morphology of copolymers can be easily tuned from micelle to hollow sphere by varying the concentration and solvent, and importantly the sizes of nanostructures by TEM matched well with those of DLS analysis.

As seldom report regarding the dielectric property of PA-contained polymers, we thus made a systematic investigation on the dielectric behavior of **PFNDI**, **PFNP**, and **PFNP-*b*-PFHD** with different weight fraction of **PFHD** block as a function of frequency at room temperature. By dispersing copolymers in selective solvent of $CHCl_3$ and spin-coating the solution on ITO substrate, a core-shell nanostructure will be saved in polymer film, resulting in excellent dielectric performance, and the results are summarized in Table S3 (ESI†). **PFNDI** with mixed *trans*/*cis* and irregular backbone has a low permittivity of 5 and relatively low dielectric loss of 0.05-0.06 as

common polymer dielectrics. However, after the reduction of pendant dicartboxyimide to pyrrolidine, the dielectric response of **PFNP** was raised to 11 and dielectric loss was still at 0.04-0.06. The dielectric performance of **PFNP** came from the orientational polarization of side chain and is closely related to its chain microstructure.[18] Compared with the dicarboxyimide structure, the electron-donating pyrrolidine moiety connecting to the electron-withdrawing bifluorophenyl moiety in **PFNP** may lead to further delocalization of electrons, enhancing dipole moment. Meanwhile, it is easy for the rigid pyrrolidine to align coherently in one orientation during ROMP process, generating **PFNP** backbone with all-*trans* and regular configuration, which is benefit for the positive accumulation of dipole moment during the orientation of polar pendants under electric field.[18] The dielectric loss mostly came from the motion of side polar groups on polymer chain under electric field below the glass transition temperature.[6]

For the traditional percolative composites, the variation of dielectric permittivity (K_c) with the conductive filler content (*f*) has been predicted to follow a critical behavior:[11] $K_c = K_m[(f_c\text{-}f)/f]^{-q}$, where K_m is the dielectric constant of the matrix, q is a critical exponent, and f_c is the percolation threshold for the conduction. When *f* increased approaching to f_c, the connected particles tend to form a conduction pathway along the percolated conductive/insulative interface, resulting in a sharply increase in K_c as well as a high dielectric loss and early electric breakdown. According to the equation, **PFNP**, with a relatively high K_m, was chosen as the insulated block to make sure a high K_c when the proportion of **PFHD** block (*f*) was not close to the threshold (f_c). Obviously, copolymers possessed higher K_c (Fig. 3a) and lower dielectric loss (Fig. 3b) than homopolymer. For copolymers with a fixed **PFNP** length of 75 units, K_c firstly increased from 17 to 22 as the **PFHD** length varied from 15 units (19.6 wt% of **PFHD**) to 25 units (28.9 wt% of **PFHD**), and then slightly decreased to 12 as the **PFHD** length was up to 50 units (44.8 wt% of **PFHD**) (Fig. S12, ESI†). When it comes to **PFNP**$_{50}$-*b*-**PFHD**$_{25}$ (37.8 wt% of **PFHD**), it possessed a much lower K_c of 7 even than that of **PFNP**, which was attributed to the shorter **PFNP** block in copolymer. Besides, K_c of copolymers was stable and almost free of frequency at 100 Hz-1 MHz, as an advantage over the traditional percolative composites.

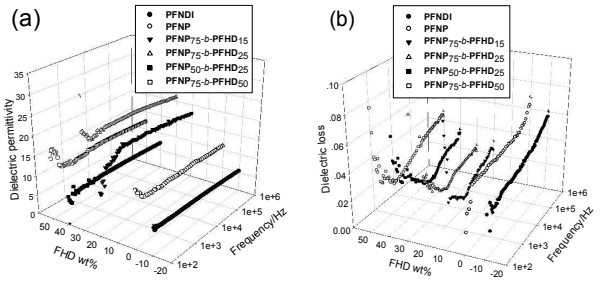

Fig. 3 Dielectric permittivity (a) and dielectric loss (b) of **PFNDI**, **PFNP**, and **PFNP**$_n$-*b*-**PFHD**$_m$ versus frequency from 100 Hz to 1 MHz.

The higher K_c of copolymers came from the combined action of orientational polarization in **PFNP** block and interfacial polarization between two blocks (Fig. S13, ESI†). The variation in K_c of copolymers was affected by different interfacial polarization due to varied contents of conductive block. Particularly, the unique core-shell nanostructure plays an important role to improve dielectric performance of materials. Firstly, under electric field, large interfacial areas between the conductive core and the insulating shell promote the accumulation of space charge and high interfacial polarization, resulting in the formation of a microcapacitor for every micelle and ultimately leading to improved dielectric response of materials. When the *f* increased, more space charge was generated along the interface and the K_c increased correspondingly.[2a] Secondly, the conductive **PFHD** core was inhibited by the insulating **PFNP** shell and hard to associate with each other, and thus dielectric dissipation is tiny and no obvious percolation was observed when the content of conductive **PFHD** (*f*) increased from 19.6 to 44.8 wt%. However, the lower K_c may mostly come from the reduced quality of polymer film with a higher *f* of 44.8 wt% **PFHD**, since **PFHD** is a rigid block with bad film-forming property, which was confirmed by SEM micrographs (Fig. S14, ESI†). Thirdly, nano-scale domains of conductive **PFHD** core would allow sufficiently fast polarizable response under high frequency electric fields, leading to K_c of copolymers as stable as that of homopolymer **PFNP**. Lastly, the conductive core and insulated shell were connected by the covalent bond, which improves their compatibility and decreases the dissipation caused by the defect on the interface.[15] Therefore, the dielectric loss mainly came from the current dissipation within every conductive **PFHD** core, and increased in consistence with *f*.

Copolymers with unique core-shell nanostructrue showed not only good dielectric properties at low electric field, but also improved breakdown field and energy density, which were also investigated by the electric displacement (D)–electric field (E) hysteresis loop measurement for polymer film. The maximum field strength was about 200 MV m^{-1} for copolymers or over this value for **PFNP** through I-V test, which was very competitive since the breakdown field always below 20 MV/m for the percolative materials.[9c,24] According to this, polarization loops were obtained with increased field strength up to 200 MV m^{-1}. The polarization of all polymers is much higher than that of commercial BOPP capacitor film under the same applied electric field (less than 0.50 μC cm^{-2} at 200 MV m^{-1}).[1c] Additionally, **PFNP** (Fig. S15a, ESI†) and **PFNP**-*b*-**PFHD** (Fig. 4a-4c) exhibited a linear polarization behavior (narrow linear D-E loops) under the relatively low applied electric field (< 60 MV m^{-1}). The linear polarization behavior and low hysteresis observed for copolymers indicated the low levels of energy dissipation, which were in good agreement with the low dielectric loss in impendence test. When the maximum applied electric field was enhanced up to 200 MV m^{-1}, **PFNP** maintained low hysteresis, while copolymers exhibited slightly tilted up D-E loops, due to the increasing leakage of electric current inside **PFHD** domains. The obvious leakage of **PFNP**$_{75}$-*b*-**PFHD**$_{50}$ also came from the bad film quality since the elongated **PFHD** fraction is hard, resulting in defects or air voids in the film (Fig. S14b, ESI†). At fixed field strength, the polarization of copolymers increased with increasing **PFHD** wt%. The energy density (U_e) of a capacitor is given by the equation:[3] $U_e = \int E(dD)$, where *E* and *D* are the applied electric field and electric displacement, respectively. According to this equation, the stored or released energy density of polymers as a function of the maximum electric field strength could be obtained by integrating charge or discharge curve of D–E loop. Evidently, the energy density for **PFNP**-*b*-**PFHD** increased as the **PFHD** block content increase (Fig. 4d-4f), and copolymers possess a higher

energy density than **PFNP** (Fig. S15b, ESI†). However, this is accompanied by an increase in energy loss (the area enclosed by the charge–discharge cycle) due to current leakage inside conductive **PFHD** domains, and the dissipative energy during charge and discharge cycles may be disadvantage in application. Specifically, for **PFNP**$_{75}$-*b*-**PFHD**$_{50}$, the stored energy density was up to 1.34 J cm^{-3}, which was about 33% greater than that of **PFNP**$_{75}$-*b*-**PFHD**$_{25}$ (1.01 J cm^{-3}) and 42% greater than that of **PFNP**$_{75}$-*b*-**PFHD**$_{15}$ (0.95 J cm^{-3}) under 200 MV m^{-1} field; however, its released energy density of just 0.90 J cm^{-3} is almost the same as **PFNP**$_{75}$-*b*-**PFHD**$_{25}$ (0.90 J cm^{-3}) and **PFNP**$_{75}$-*b*-**PFHD**$_{15}$ (0.89 J cm^{-3}) under 200 MV m^{-1} field. In general, the energy density of copolymer is almost the same as the best value of reported percolative materials with oligoaniline or oligothiophene as conductive segments at the similar molecule weight. However, limited by the rigid conductive **PFHD** backbone, the energy dissipation is inevitable and higher than that of polymers with oligo-conductive side chains.[2a,12a,24] Comparing to **PFNP**$_{75}$-*b*-**PFHD**$_{50}$, **PFNP**$_{75}$-*b*-**PFHD**$_{25}$ and **PFNP**$_{75}$-*b*-**PFHD**$_{15}$ may be better candidates for polymer dielectric material with high stored/released energy density, high breakdown field, and low dissipation at room temperature.

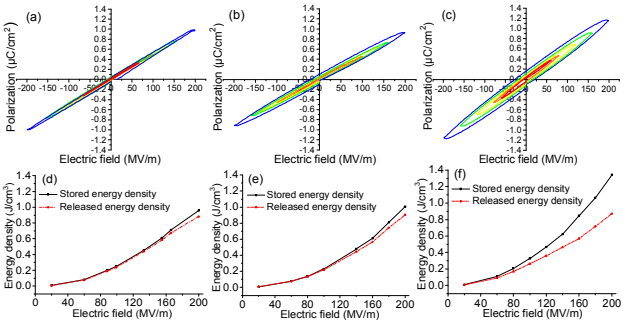

Fig. 4 Polarization (D–E) loops (top) and energy density versus applied electric field (down) for (a, d) **PFNP**$_{75}$-*b*-**PFHD**$_{15}$, (b, e) **PFNP**$_{75}$-*b*-**PFHD**$_{25}$, and (c, f) **PFNP**$_{75}$-*b*-**PFHD**$_{50}$.

In conclusion, a new type of insulating-conductive block copolymer **PFNP**-*b*-**PFHD** was synthesized by a tandem ROMP-MCP procedure, which has the ability to form a stable core-shell micelle or hollow sphere nanostructure through the self-assembly in selective solvent. The conductive **PFHD** core is enwrapped by the insulating **PFNP** shell for effectively inhibiting the current leakage, even though the micelles aggregated. The combination of the high permanent dipole of **PFNP** and the favorable interfacial polarization between the conductive core and the insulated shell endows this novel material high dielectric permittivity and energy density, as well as low dielectric dissipation. This research is expected to present a facile way to achieve nanodielectric materials with tunable nanostructure and excellent performance.

The research was financially supported by the National Natural Science Foundation of China (No. 21374030, 21074036).

Notes and references

1 (a) W. Sarjeant, I. W. Clelland and R. A. Price, *Proc. IEE,* 2001, **89**, 846; (b) L. Zhu and Q. Wang, *Macromolecules,* 2012, **45**, 2937; (c) G. J. Reynolds, M. Kratzer, M. Dubs, H. Felzer and R. Mamazza, *Materials,* 2012, **5**, 575.

2 (a) C. G. Hardy, M. S. Islam, D. Gonzalez-Delozier, J. E. Morgan, B. Cash, B. C. Benicewicz, H. J. Ploehn and C. Tang, *Chem. Mater.,* 2013, **25**, 799; (b) S. P. Fillery, H. Koerner, L. Drummy, E. Dunkerley, M. F. Durstock, D. F. Schmidt and R. A. Vaia, *ACS Appl. Mater. Interfaces,* 2012, **4**, 1388.

3 B. Chu, X. Zhou, K. Ren, B. Neese, M. Lin, Q. Wang, F. Bauer and Q. M. Zhang, *Science,* 2006, **313**, 334.

4 W. Hao, J. Zhang, Y. Tan, M. Zhao and C. Wang, *J. Am.Chem. Soc.,* 2011, **94**, 1067.

5 (a) Q. Zhang, V. Bharti and X. Zhao, *Science,* 1998, **280**, 2101; (b) Q. Zhang, H. Li, M. Poh, F. Xia, Z. Y. Cheng, H. Xu and C. Huang, *Nature,* 2002, **419**, 284; (c) S. Wu, M. Lin, S. G. Lu, L. Zhu and Q. M. Zhang, *Appl. Phys. Lett.,* 2011, **99**, 132901.

6 J. Wei, Z. Zhang, J. K. Tseng, I. Treufeld, X. Liu, M. H. Litt and L. Zhu, *ACS Appl. Mater. Interfaces,* 2015, **7**, 5248.

7 (a) D. H. Wang, B. A. Kurish, I. Treufeld, L. Zhu and L. S. Tan, *J. Polym. Sci., Part A: Polym. Chem.,* 2015, **53**, 422; (b) M. Inutsuka, K. Inoue, Y. Hayashi, A. Inomata, Y. Sakai, H. Yokoyama and K. Ito, *Polymer,* 2015, **59**, 10.

8 (a) K. Yang, X. Huang, Y. Huang, L. Xie and P. Jiang, *Chem. Mater.,* 2013, **25**, 2327; (b) K. Yang, X. Huang, M. Zhu, L. Xie, T. Tanaka and P. Jiang, *ACS Appl. Mater. Interfaces,* 2014, **6**, 1812.

9 (a) H. Quan, D. Chen, X. Xie and H. Fan, *Phys. Status Solidi., A* 2013, **210**, 2706; (b) L. Qi, B. I. Lee, S. Chen, W. D. Samuels and G. J. Exarhos, *Adv. Mater.,* 2005, **17**, 1777; (c) C. A. Grabowski, S. P. Fillery, N. M. Westing, C. Chi, J. S. Meth, M. F. Durstock and R. A. Vaia, *ACS Appl. Mater. Interfaces,* 2013, **5**, 5486.

10 C. Huang and Q. Zhang, *Adv. Funct. Mater.,* 2004, **14**, 501.

11 (a) S. Liang, J. Claude, K. Xu and Q. Wang, *Macromolecules,* 2008, **41**, 6265; (b) M. Molberg, D. Crespy, P. Rupper, F. Nüesch, J. A. E. Månson, C. Löwe and D. M. Opris, *Adv. Funct. Mater.,* 2010, **20**, 3280.

12 (a) Y. Qiao, M. S. Islam, K. Han, E. Leonhardt, J. Zhang, Q. Wang, H. J. Ploehn and C. Tang, *Adv. Funct. Mater.,* 2013, **23**, 5638; (b) Y. Qiao, M. S. Islam, X. Yin, K. Han, Y. Yan, J. Zhang, Q. Wang, H. J. Ploehn and C. Tang, *Polymer,* 2015, **72**, 428.

13 (a) M. N. Almadhoun, M. N. Hedhili, I. N. Odeh, P. Xavier, U. S. Bhansali and H. N. Alshareef, *Chem. Mater.,* 2014, **26**, 2856; (b) B. Li and W. H. Zhong, *J. Mater. Sci.,* 2011, **46**, 5595.

14 (a) R. R. Kohlmeyer, A. Javadi, B. Pradhan, S. Pilla, K. Setyowati, J. Chen and S. Gong, *J. Phys. Chem. C.,* 2009, **113**, 17626; (b) J. K. Yuan, S. H. Yao, Z. M. Dang, A. Sylvestre, M. Genestoux and J. Bai1, *J. Phys. Chem. C.,* 2011, **115**, 5515.

15 F. Wen, Z. Xu, S. Tan, W. Xia, X. Wei and Z. Zhang, *ACS Appl. Mater. Interfaces,* 2013, **5**, 9411.

16 B. Liu, Y. Li, A. S. Mathews, Y. Wang, W. Yan, S. Abraham, C. S. Ha, D. W. Park and I. Kim, *React. Funct. Polym.,* 2008, **68**, 1619.

17 G. Davies, H. S. A. Hubbard, I. Ward, W. Feast, V. Gibson, E. Khosravi and E. Marshall, *Polymer,* 1995, **36**, 235.

18 (a) Z. You, D. Gao, O. Jin, X. He and M. Xie, *J. Polym. Sci., Part A: Polym. Chem.,* 2013, **51**, 1292; (b) G. R. Davies, H. V. St. A. Hubbard and I. M. Ward, *Polymer,* 1995, **36**, 235.

19 (a) U. Anders, M. Wagner, O. Nuyken and M. R. Buchmeiser, *Macromolecules,* 2003, **36**, 2668; (b) E. H. Kang, S. Y. Yu, I. S. Lee, S. E. Park and T. L. Choi, *J. Am. Chem. Soc.,* 2014, **136**, 10508.

20 (a) C. Wu, A. Niu, L. M. Leung and T. Lam, *J. Am. Chem. Soc.,* 1999, **121**, 1954; (b) S. Shin, K. Y. Yoon and T. L. Choi, *Macromolecules,* 2015, **48**, 1390.

21 H. Shirakawa, *Angew. Chem., Int. Ed.,* 2001, **40**, 2574.

22 a) A. J. Heeger, *Angew. Chem., Int. Ed.,* 2001, **40**, 2591; (b) S. K. Choi, Y. S. Gal, S. H. Jin and H. K. Kim, *Chem. Rev.,* 2000, **100**, 1645.

23 (a) E. H. Kang, I. H. Lee and T. L. Choi, *ACS Macro Lett.,* 2012, **1**, 1098; (b) J. O. Krause, M. T. Zarka, U. Anders, R. Weberskirch, O. Nuyken and M. R. Buchmeiser, *Angew. Chem., Int. Ed.,* 2003, **42**, 5965.

24 M. S. Islam, Y. Qiao, C. Tang and H. J. Ploehn, *ACS Appl. Mater. Interfaces,* 2015, **7**, 1967.